The chemistrode: A droplet-based microfluidic device for stimulation and recording with high temporal, spatial, and chemical resolution

Delai Chen[a,1], Wenbin Du[a,1], Ying Liu[a,1], Weishan Liu[a,1], Andrey Kuznetsov[b], Felipe E. Mendez[b], Louis H. Philipson[b], and Rustem F. Ismagilov[a,2]

[a]Department of Chemistry and Institute for Biophysical Dynamics, University of Chicago, 929 East 57th Street, Chicago, IL 60637; and [b]Department of Medicine and the Kovler Diabetes Center, University of Chicago, 5841 South Maryland Avenue, Chicago, IL 60637

Edited by George M. Whitesides, Harvard University, Cambridge, MA, and approved September 15, 2008 (received for review August 19, 2008)

Microelectrodes enable localized electrical stimulation and recording, and they have revolutionized our understanding of the spatiotemporal dynamics of systems that generate or respond to electrical signals. However, such comprehensive understanding of systems that rely on molecular signals—e.g., chemical communication in multicellular neural, developmental, or immune systems—remains elusive because of the inability to deliver, capture, and interpret complex chemical information. To overcome this challenge, we developed the "chemistrode," a plug-based microfluidic device that enables stimulation, recording, and analysis of molecular signals with high spatial and temporal resolution. Stimulation with and recording of pulses as short as 50 ms was demonstrated. A pair of chemistrodes fabricated by multilayer soft lithography recorded independent signals from 2 locations separated by 15 μm. Like an electrode, the chemistrode does not need to be built into an experimental system—it is simply brought into contact with a chemical or biological substrate, and, instead of electrical signals, molecular signals are exchanged. Recorded molecular signals can be injected with additional reagents and analyzed off-line by multiple, independent techniques in parallel (e.g., fluorescence correlation spectroscopy, MALDI-MS, and fluorescence microscopy). When recombined, these analyses provide a time-resolved chemical record of a system's response to stimulation. Insulin secretion from a single murine islet of Langerhans was measured at a frequency of 0.67 Hz by using the chemistrode. This article characterizes and tests the physical principles that govern the operation of the chemistrode to enable its application to probing local dynamics of chemically responsive matter in chemistry and biology.

analysis | dispersion | flow | microscale | pulse

This article describes the "chemistrode," a droplet-based microfluidic device for manipulating and observing molecular signals with high spatial and temporal resolution. The microelectrode, voltage-clamp, and patch-clamp techniques (1) enabled stimulation and recording of electrical activity and redox-active molecules with high resolution in both space and time, revolutionizing our understanding of electroactive processes from biochemistry to neuroscience (1–3). Most biological processes, however, are fundamentally chemical rather than electrical, relying on molecular signals to orchestrate events at the correct time and location. Electrochemical approaches are widely used, but not all molecules are electrochemically active, and some electrochemically active molecules are difficult to measure selectively in complex mixtures. The grand challenge this article addresses is that of devising an analogue of the electrode that operates on molecular rather than electrical or electroactive signals.

Why could we not build such a system with today's technology? Whereas electrical signals travel through wires essentially instantly and with low losses, manipulation and transport of molecules is more challenging. First, a pulse of molecules, especially of small volume, rapidly disperses when transported through a tube by laminar flow, leading to loss of concentration and time resolution. Loss of molecules from solution by adsorption to surfaces of tubes may also occur. Therefore, methods that rely on laminar flow to transport molecular signals, such as direct sampling (4), push/pull perfusion (5), microdialysis (6), and direct microinjection, have not addressed this grand challenge. In contrast to electrical signals, molecular signals comprise multiple, often unknown, molecular species, requiring the ability to deliver multiple molecular species as stimuli and the ability to analyze a pulse of response molecules by multiple techniques. Advances in optical imaging technology, new probes and tagging methods, and photo-controllable manipulation have enabled observation and manipulation of many known molecular species, but these technologies may be time consuming to develop for each species and difficult to use for multiple or unknown species. "Biology on a chip" microfluidics technologies (7–9) can reduce dispersion by minimizing the distance that molecules are transported by the integration of a biological experiment with a specific analytical method. However, this approach requires the redevelopment and validation of the biological protocols as well as the miniaturization and integration of disparate analytical technologies. Recent advances in microfluidics have used multiphase flow to transport solutions reliably as discrete units without dilution, cross-contamination, or loss of temporal resolution (10–19).

We developed the chemistrode, a microfluidic platform that addresses this grand challenge by providing molecular stimulation and recording with high fidelity using plug-based (12) multiphase microfluidics [Fig. 1*A* and supporting information (SI) Fig. S1]. Like the electrode, the chemistrode is simply brought into contact with the surface under investigation, e.g., a cell or tissue. Instead of exchanging electrical signals, molecular signals are delivered by and captured in plugs, aqueous droplets nanoliters in volume surrounded by a fluorocarbon carrier fluid. The compartmentalization of these molecular signals eliminates dispersion and loss of sample due to surface adsorption (18).

Operation of the chemistrode relies on 9 general steps (Fig. 1 *A* and *B*): (*i*) preparation of an array of aqueous plugs containing an arbitrary sequence of stimuli (20, 21); (*ii*) delivery of the array of stimulus plugs to a hydrophilic substrate; (*iii*) coalescence of

Author contributions: D.C., W.D., Y.L., W.L., A.K., L.H.P., and R.F.I. designed research; D.C., W.D., Y.L., W.L., and F.E.M. performed research; D.C., W.D., Y.L., W.L., A.K., L.H.P., and R.F.I. analyzed data; and D.C., W.D., Y.L., W.L., and R.F.I. wrote the paper.

The authors declare no conflict of interest.

This article is a PNAS Direct Submission.

[1]D.C., W.D., Y.L., and W.L. contributed equally to this work.

[2]To whom correspondence should be addressed. E-mail: r-ismagilov@uchicago.edu.

This article contains supporting information online at www.pnas.org/cgi/content/full/0807916105/DCSupplemental.

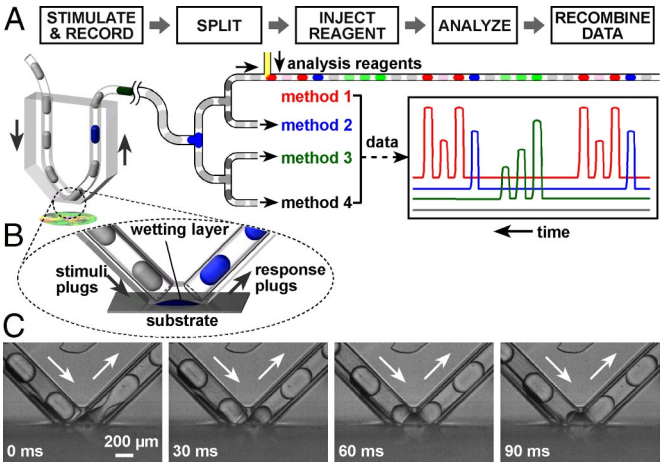

Fig. 1. The chemistrode delivers and records multiple molecular signals with high temporal and spatial resolution for off-line analysis by multiple analytical methods in parallel. (*A*) A conceptual schematic drawing of stimulation, recording, and analysis. See text for details. (*B*) Schematic of the chemistrode brought into contact with a hydrophilic substrate. (*C*) Time-lapse bright-field images (side view) of an incoming stimulus plug merging with the wetting layer above a hydrophilic glass surface and the formation of a response plug as the fluid exits the wetting layer (see Movie S1).

stimulus plugs with the wetting layer above the hydrophilic substrate (11) while the fluorocarbon carrier fluid remains in contact with the hydrophobic wall of the chemistrode; (*iv*) rapid exchange of diffusible signals between the plug and the wetting layer; (*v*) re-formation of plugs containing response molecules released by the substrate; (*vi*) delivery of response plugs to a splitting junction to form identical daughter arrays (22); (*vii*) injection of each daughter array with reagents required for further analysis (23); (*viii*) analysis of each daughter array by a different technique; and (*ix*) final recombination of data from the analysis of daughter arrays to provide a time-resolved record of molecular stimulation and response dynamics. Here, we describe the physical principles that guide the operation of the chemistrode and implement the chemistrode to test the feasibility of each step and the compatibility of this platform with living cells.

Results

To deliver pulses of stimuli and capture pulses of molecular signals as they are released with high temporal resolution and efficiency, the chemistrode must handle plugs at high frequency while ensuring coalescence of plugs with the wetting layer and efficient chemical exchange between a plug and the wetting layer. To characterize these parameters, we fabricated a chemistrode with a v-shaped channel (with 200- or 240-μm i.d. Teflon tubing inserted) by using rapid prototyping in poly(dimethylsiloxane) (PDMS) (Fig. 1*B* and Fig. S1) (24). Microchannels were rendered hydrophobic and fluorophilic by using silanization (25). By using high-speed video microscopy, steps *ii* through *v* were observed for the delivery and recording of buffer plugs on a hydrophilic glass surface (Fig. 1*C*). To achieve stable transport of plugs, the chemistrode must operate at a low value of the capillary number, $Ca = U\mu/\gamma < 0.1$, where U (m/s) is the flow velocity, μ (kg/m·s) is the dynamic viscosity, and γ (N/m) is the surface tension at the interface between the aqueous phase and the carrier fluid (26). Assuming the center-to-center distance between adjacent plugs to be 6 times d (m), the diameter of the channel (26), Ca limits the frequency f at which plugs can flow over a surface, f_{Ca} (s^{-1}), to $\frac{Ca\cdot\gamma}{\mu\cdot 6d}$, or $f_{Ca} \approx 0.17(\text{m/s})/d$. For the channels of the chemistrode used here, $d = 2 \times 10^{-4}$ m, corresponding to $f_{Ca} \approx 800\ s^{-1}$.

The pressure drop, ΔP (Pa), required to achieve these frequencies provides an additional constraint on frequency, $f_{\Delta P}$. By using the Hagen–Poiseuille equation as an approximation, for a channel with length L (m) long enough to hold N plugs, $L = 6Nd$, and $f_{\Delta P} = \frac{\Delta P}{6N \times 192\ \mu}$, independent of d. When $n = 100$ and $\Delta P \approx 10^5$ Pa, $f_{\Delta P} \approx 900\ s^{-1}$, but this value is the upper bound of $f_{\Delta P}$, because multiphase flow requires higher pressure drops than predicted by the Hagen–Poiseuille equation because of capillary pressure, Marangoni stresses, and a modification of the velocity profile inside the plugs (27).

To achieve rapid coalescence of the stimulus plug and the wetting layer (step *iii*), 3 factors must be considered (11, 28): (*i*) the rate of drainage of the carrier fluid to bring the wetting layer and the plug within a critical distance for coalescence, (*b*) the critical contact time between the wetting layer and the plug at the critical distance, and (*c*) surfactant dynamics (29, 30). Geometry of the chemistrode prevented the fusion of multiple droplets on the surface and chemical exchange among them. Although such fusion is a useful feature in some applications (11), it is undesirable for the chemistrode, because fusion introduces cross-contamination and reduces temporal resolution. We accelerated coalescence by using carrier fluids with low viscosity that can drain on the submillisecond time scale. We also used a small-molecule surfactant, triethyleneglycol mono[1H,1H-perfluorooctyl]ether (RfOEG) known to prevent nonspecific protein adsorption (25) to the aqueous–fluorous interface. This surfactant induced desirable surface tension and displayed sufficiently rapid dynamics to provide reliable frequencies of coalescence, $f_{coal} > 50\ s^{-1}$. By considering the parameters and conditions described above, the temporal resolution, t_{res} (s), can be estimated as $t_{res} \approx \frac{\phi}{f}$, where f is the limiting frequency (the lowest one among f_{Ca}, $f_{\Delta P}$, and f_{coal}), and ϕ is the unitless number of plugs necessary to exchange >95% of molecules of interest between plugs and the wetting layer (which was in the $\approx 10^1$- to 10^2-μm range in our experiments, depending on the geometry and flow rate).

To test the efficiency of chemical exchange between plugs and the wetting layer (step *iv*), high-speed fluorescence video microscopy was used to observe a fluorescent molecular signal delivered to a hydrophilic glass surface (Fig. 2*A*). We used small-molecule fluorescent dyes for simplicity and because many diffusible signals are small molecules. The fluorescent signal was encoded in 1 plug containing fluorescein, which was followed by many plugs of nonfluorescent buffer. This array was flowed into the chemistrode at a flow velocity of 4.2 mm/s, and an increase in fluorescence at the surface of the substrate was observed after the fluorescent plug coalesced with the wetting layer. The fluorescein in the wetting layer was rapidly removed by subsequent buffer plugs with $\phi = 3$ (Fig. 2*A*). Experimentally, the observed value of ϕ depended on the extent of recirculation induced as plugs coalesced with the wetting layer. The value of ϕ correlated with the value of $\sqrt{We}$, the square root of the dimensionless Weber number (24), which describes the ratio of fluid's inertia to surface tension driving recirculation (data not shown). $We = \rho U^2 d/\gamma$, where ρ (kg/m^3) is the density of the fluid. We quantified this effect by using the chemistrode to deliver an array of plugs of fluorescein to saturate the wetting layer, followed by an array of buffer plugs that removed fluorescein from the wetting layer (Fig. 2*B* and Fig. S2). As $\sqrt{We}$ increased from 0.0036 to 0.14, recirculation was reduced, and the value of ϕ decreased from 4 to 2. Viscosity of the plugs did not significantly affect the value of ϕ (data not shown), also suggesting that $\sqrt{We}$ is better than Ca or Re for describing ϕ. Mass transport by

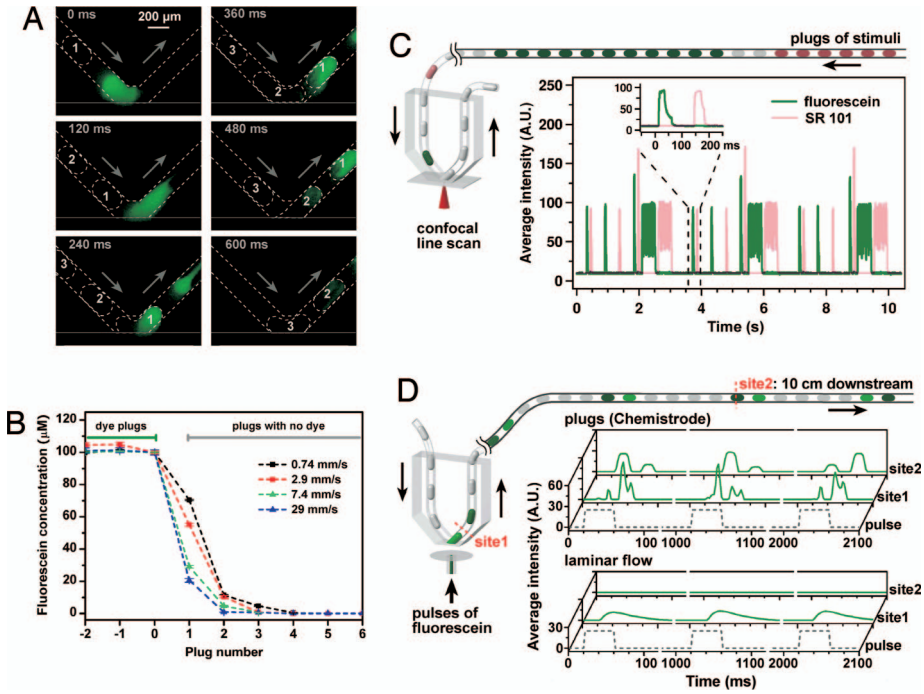

Fig. 2. The chemistrode provides stimulation and recording with high temporal resolution. (*A*) Time-lapse fluorescence images of the delivery and capture of fluorescein within the wetting layer by 3 buffer plugs. See Movie S2 for more details. (*B*) Removal of fluorescein from the wetting layer by buffer plugs as a function of flow velocity. Data indicate rapid mass transport between the wetting layer and the plugs. Error bars are standard deviation ($n = 5$) (see *SI Text*). (*C*) Stimulation with a preformed array of fluorescent plugs containing fluorescein (green), sulforhodamine 101 (red), and buffer (gray) detected at the wetting layer with a confocal microscope (schematic on the left, experimental data on the right). A.U., arbitrary units. (*D*) Intensity of recorded 40-ms pulses of fluorescein measured at the tip of the chemistrode (site 1) and 10 cm downstream (site 2) (schematic on the left). Experimental data (right, green graphs of fluorescence intensity) show that pulses (shown as dashed gray lines) are reliably captured at site 1 and transported 10 cm to site 2 by response plugs in the chemistrode (upper graph and Movie S3) but not by the single-phase laminar flow in the same device (lower graph and Movie S4).

diffusion near the surface did not limit the overall mass transport in those experiments, but it could become limiting for molecules with very low effective diffusion coefficients (e.g., because of large size or binding to cell surfaces or extracellular matrix). For systems where both mass transport and kinetics are slow, the flow may be stopped and restarted to allow plugs to collect more of the released molecules. Overall, these experiments predicted that a temporal resolution of ≈50 ms should be achievable in this geometry at higher flow velocities. Re-formation of response plugs (step *v*) took place reliably in the chemistrode at $Ca < 0.1$ and did not limit t_{res}.

Using the parameters described above, the chemistrode enabled delivery of an array of an arbitrary sequence of multiple molecular signals as pulses of controlled intensity and duration at high temporal resolution (Fig. 2*C* and Fig. S3). We delivered plugs of only 2 fluorescent dyes and imaged the wetting layer with 2 wavelengths simultaneously by using high-speed confocal microscopy. Short pulses with duration of ≈50 ms (width at half-height) were encoded in individual plugs, delivered at a frequency of 1 plug per 50 ms. Because long plugs may break up spontaneously, encoding of longer pulses was more reliable with sequences of short plugs. Higher-intensity pulses were encoded with plugs containing the reagent at higher concentration. The predetermined sequence of plugs was delivered 3 times with high reproducibility (Fig. 2*C*). This experiment confirmed efficient delivery of the reagents into the wetting layer, also observed in Fig. 2*A*. These results also demonstrated that the chemistrode is compatible with standard optical imaging techniques.

We hypothesized that the chemistrode would provide efficient recording of released signals superior to that of single-phase laminar flow. To simulate the release of molecules from a surface, fluorescein was pulsed out of a glass microcapillary tube that ended flush with the PDMS surface (Fig. 2*D*). The chemistrode was brought into contact with the wetting layer above the tip of the capillary tube. Pulses of ≈40 ms with a volume of 0.2 nL were generated every second and collected by using either the plug-based flow (at a frequency of 1 plug per ≈37 ms) of the chemistrode or single-phase laminar flow in the same geometry (Fig. 2*D* and Fig. S4). Fluorescence was detected at the tip of the device (site 1) and 10 cm downstream (site 2) by using high-speed fluorescence video microscopy. In these experiments, we were unable to measure fluorescence simultaneously at both sites. Therefore, the plots of fluorescence intensity shown for sites 1 and 2 are sequential but do not correspond to the same pulses. In the chemistrode at site 1, >95% of the fluorescent signal was distributed over no more than 2 plugs. Recirculation within plugs redistributed the contents of the pulse and caused the measured signal to fluctuate in some of the plugs (Movie S3). The recorded signal was transported 10 cm with no loss of temporal resolution. In contrast, recording with single-phase laminar flow resulted in poor temporal resolution and poor efficiency of collection. Broadening of the fluorescent peaks was already visible at the tip of the device (site 1, Movie S4), and the intensity of the signal decreased to <1% of the initial value after traveling 10 cm downstream (site 2) because of dispersion.

To test whether the chemistrode provided chemical stimulation and recording with spatial resolution of tens of micrometers—potentially important for work on the cellular and subcellular scales—we used multilayer soft lithography (31, 32) to fabricate a 2-layer chemistrode with 25-μm channels separated by a thin (15 μm) spacer of PDMS (Fig. 3*A* and Fig. S5). To simulate the release of molecules from a hydrophilic surface at 2 locations, we ejected pulses of any of 3 solutions through 2 (30 ± 2) × (20 ± 5)-μm orifices separated by 15 μm (Fig. 3*A*).

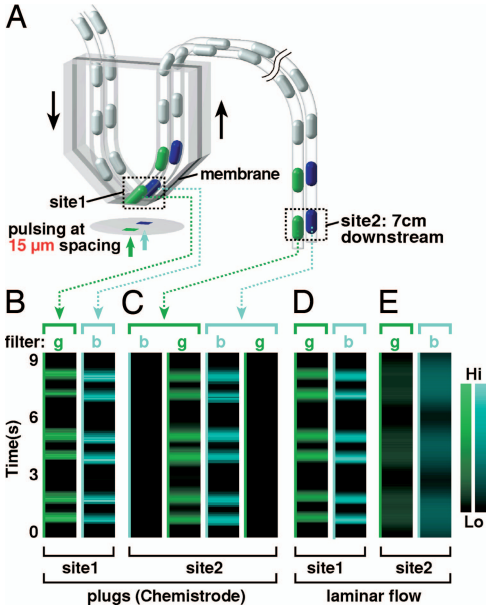

Fig. 3. An array of chemistrodes operates at high spatial resolution. (*A*) A schematic drawing of the 2-layer chemistrode device used for sampling 2 signals, 8-methoxypyrene-1,3,6 trisulfonic acid (MPTS, blue) or fluorescein (green), released through 2 orifices separated by 15 μm (see *SI Text*). (*B–E*) A plot of fluorescence intensity of the 2 fluorescent signals, observed through green (g) and blue (b) filters, captured and transported by plugs of the chemistrode (*B* and *C*) and laminar flow (*D* and *E*) in the same geometry.

The solutions were buffer (colorless), fluorescein (green), and 8-methoxypyrene-1,3,6 trisulfonic acid (MPTS, blue). We then brought the pair of chemistrodes in contact with the wetting layer above the orifices to record ejected pulses, and we detected fluorescence at the tip of the device (site 1) and 7 cm downstream (site 2). The 2-layer chemistrode reliably recorded the sequences of pulses at both locations (Fig. 3 *B* and *C*) with cross-contamination of $<1\%$ and no loss of intensity during transport (Fig. 3*C*). The use of plugs was essential—when single-phase laminar flow was used instead, pulses rapidly broadened, overlapped, and decayed (Fig. 3 *D* and *E*). In these small channels, Taylor dispersion was less severe, but losses to the walls of channels became pronounced, especially when we tested solutions of proteins. Because the carrier fluid completely encapsulates the aqueous plug and eliminates its contact with the walls, two-phase flow of the chemistrode reliably transported even molecules that tended to adsorb to PDMS and Teflon. We do not anticipate partitioning of hydrophobic or amphiphilic molecules from the aqueous plugs into the fluorocarbon carrier fluid, as shown in previous studies (33, 34).

To test the compatibility of the chemistrode with off-line, multianalyte measurements by independent methods (steps *vi–ix*), we used the chemistrode to record pulses of a mixture of 4 compounds—$CaCl_2$, insulin, glucose, and MPTS as a positive control—each representing a different class of molecules and detectable by a different technique (Fig. 4*A*). A mixture of these compounds was pulsed through the end of a Y-shaped channel. The chemistrode was brought into contact with the wetting layer above the channel. The array of recorded response plugs was split into 4 identical daughter arrays (step *vi*). Each plug in the first daughter array was injected (step *vii*) with a fluorescent indicator, fluo-4. Measuring fluorescence of the fluo-4-Ca^{2+} complex of each plug (step *viii*) in this array detected the presence of Ca^{2+} ions and provided a profile of Ca^{2+} release as a function of time (Fig. S6). In parallel, plugs in the second array were injected with the mixture of an anti-insulin antibody and labeled insulin for a competitive immunoassay with a 20 nM limit of detection, shown as the baseline in Fig. 4*B* and Fig. S7. Control experiments indicated that plugs provide an excellent transport and storage medium for insulin for off-line analysis with no losses of insulin due to degradation or adsorption to surfaces (25), in contrast to almost complete loss of insulin from laminar flow in the same Teflon tube. To determine the concentration of insulin, the fraction of labeled insulin that was free or bound to the antibody was detected by using fluorescence correlation spectroscopy (FCS) (35). Plugs in the third array were injected with Girard's reagent T [(carboxymethyl)trimethylammonium chloride hydrazide] and incubated overnight to give a hydrazone derivative of glucose, and the presence of the hydrazone was then detected by MALDI-MS (Fig. S8, a method that can detect unknown molecules. As a control, fluorescence of MPTS was measured in the fourth array. Analysis of insulin data indicated that $>98\%$ of the pulsed signal was recovered by the chemistrode. Final recombination of data from all 4 analyses (step *ix*) showed good alignment among different techniques and with the positive control trace of MPTS (Fig. 4*B*).

Splitting followed by off-line analysis (Fig. 4*A*) is an attractive feature of the chemistrode that decouples the stimulating and recording experiment from the equipment and expertise that may be required for analysis of nanoliter volumes. We demonstrated decoupling in time: Whereas the chemical signals were recorded on the time scale of seconds, incubation and measurement steps during analysis required >24 h but did not lead to loss of signal or time resolution. We also demonstrated decoupling in location: We performed recording with the chemistrode (Fig. 4*A*) in our laboratory and analyzed plugs for insulin 1 day later by using an FCS instrument located 20 miles away. Control experiments indicated that storage and transportation of tubing containing response plugs did not affect the time resolution or quality of analysis by FCS. Arrays of plugs have been shipped cross-country or frozen and thawed without disruption. The ability to deliver, record with no losses of resolution or concentration, duplicate, store, send by mail, and analyze by multiple techniques space- and time-resolved chemical information encoded as an array of plugs in a tube could dramatically enhance collaborations and use of unique analytical facilities.

Finally, we tested the compatibility of the chemistrode with live-cell experiments (Fig. 4*C*) by using mouse islets of Langerhans, a model system widely studied in the context of diabetes (36–38). Using the chemistrode, we stimulated single islets (Fig. 4*D*) by using a transition from a resting buffer containing 2 mM glucose to a stimulant buffer containing 14 mM glucose. The increase of intracellular $[Ca^{2+}]_i$ by islets in response to the stimulation was optically monitored (36) by measuring the fluorescence intensity of fluo-4. We observed regularly oscillating $[Ca^{2+}]_i$ in islets being stimulated with plugs of buffer containing 14 mM glucose for up to 1 h (Fig. S9). Next, by forming recording plugs at a frequency of 0.67 s^{-1} and measuring the insulin concentration in the recording plugs, we determined, every 1.5 s, the rate of insulin secretion of an islet under stimulation with solutions containing 30 mM KCl and 2 mM glucose. We chose these conditions to ensure rapid response dynamics and rapid secretion of insulin. We included a fluorescent dye, Alexa Fluor 594, as a marker in the stimulant plugs. To align the trace of off-line analysis to the $[Ca^{2+}]_i$ data, we used the transitions of marker intensity between the baseline and the plateau as the references and kept track of the position of every plug in the recording array. The intensity of Alexa Fluor 594 measured by fluorescent microscopy during stimulation agreed well with the intensity measured by off-line analysis of recorded plugs, indicating that temporal information was preserved by plugs. Upon stimulation, after a short $\approx$2-s delay, the islet displayed the expected response—a sharp increase of $[Ca^{2+}]_i$ accompanied by a burst of insulin release within $\approx$10 s (Fig. 4*E*).

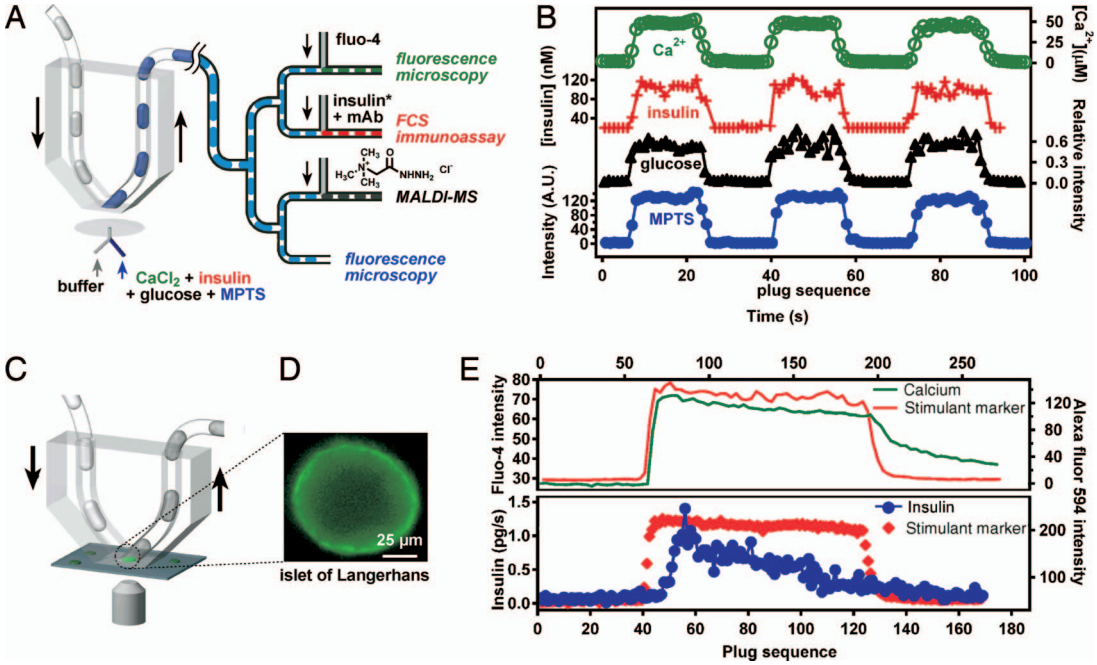

Fig. 4. The chemistrode is compatible with parallel off-line analysis by independent analytical techniques and is compatible with living cells as a substrate. (*A* and *B*): Use of the chemistrode to record and analyze pulses of sample solution containing $CaCl_2$, insulin, glucose, and a fluorescent dye, MPTS. (*A*) A schematic of the experiment. Pulses were generated at the surface. After recording with the chemistrode, recorded plugs were split into 4 identical daughter arrays for off-line analysis via fluorescence microscopy, FCS competitive immunoassay, and MALDI-MS. (*B*) Experimental data of Ca^{2+}, insulin, glucose, and MPTS analyses combined and aligned to reveal the complete release profile of the 4 species. (*C–E*) Use of the chemistrode to stimulate a mouse islet of Langerhans and record insulin secretion every 1.5 s. A.U., arbitrary units. (*C*) A schematic of the experiment. An islet was cultured on a glass-bottom dish, and the chemistrode was positioned over the islet. Stimulation and recording took place while the islet was imaged by fluorescence microscopy. (*D*) A fluorescent image of an islet showing an increase of fluorescence of fluo-4, corresponding to the rise in intracellular $[Ca^{2+}]_i$ in the islet upon stimulation. (*E*) Graphs showing the $[Ca^{2+}]_i$ response and insulin secretion of a stimulated mouse islet. (*Upper*) Traces measured by fluorescence microscopy during stimulation and recording, showing the fluorescence intensity of fluo-4 (green) as an indicator of $[Ca^{2+}]_i$ and the intensity of Alexa Fluor 594 (red) as a marker of the stimulant solution. (*Lower*) Traces with results of off-line analysis of plugs collected during recording, showing the fluorescence intensity of Alexa Fluor 594 marker and the calculated insulin secretion rate.

The peak rate of insulin secretion was in general agreement with those observed previously in islet-on-a-chip microfluidic experiments (38), and the rapid dynamics of secretion are consistent with stimulation by a solution of high KCl concentration. The response was also reproduced for different batches of healthy islets and agreed with that observed in control experiments, confirming that the chemistrode did not introduce artifacts. The compatibility of the chemistrode with live-cell experiments is consistent with compatibility of single-phase, aqueous microfluidic devices widely used in experiments with living cells (7, 8, 36), with the design of chemistrode that brings only the aqueous phase in contact with the cell, whereas the fluorocarbon remains in contact with the walls of the device, and with compatibility of fluorocarbons with living cells and tissues (39).

Discussion

One may speculate that, ultimately, the ability to contact the surface of a sample at a specific location and deliver molecular stimuli and then record, store, and analyze the pulses of molecules released in response could enable truly fascinating experiments in chemistry and biology. Molecular signals could be recorded "in stereo" from multiple locations on a surface with high spatial resolution, capturing a conversation among cells or revealing differences in secretion at different regions of the same cell. A sequence of pulses of molecular signals recorded with high temporal resolution from one cell could be played back to another cell with high fidelity or manipulated to identify the sequence of molecular signals essential to induce a particular function. These and other stimulation-recording-analysis experiments could advance areas that rely on extracellular communication, from dynamics of biofilms, to development of multicellular organisms, to signaling in neural circuits, to hormonal regulation.

The chemistrode has not yet been used to carry out such speculative experiments, because, as this article describes, there are physical principles and limitations governing the operation of the chemistrode. Obviously, many opportunities remain to further advance the chemistrode. For example, what operating ranges of the chemistrode are compatible with particular living cells and tissues? Can nanoporous membranes be integrated to control the shear experienced by the substrate while providing rapid mass transfer between the substrate and the plugs? For signaling molecules that show slow mass transfer because of binding to extracellular matrices, what are the best approaches to prevent or reverse this binding, or locally disrupt the matrices? How can pressure-sensitive valves be incorporated to balance pressure at the substrate? How can mechanically stable microprobes be fabricated for insertion into tissues? What are the best analytical techniques for each application, and what is the optimal way of integrating them? How can this approach be integrated with advances in laminar-flow-based probes (9, 40–42)? The spatial resolution of the chemistrode is not yet at the level demonstrated by carbon fiber- and nanotube-based approaches (43); how can the chemistrode be scaled down further to operate in the patch-clamp mode on a single channel or to capture single secretory vesicles? As these questions are answered, the chemistrode should advance chemistry of responsive materials (44, 45), surface catalysis (46), and understanding of biological systems that are intrinsically responsive to stimuli and display nontrivial spatial and temporal dynamics on levels ranging from networks (47) to cells (48) to tissues (49, 50).

Materials and Methods

See *SI Text* for materials, more detailed procedures, and additional data.

Fabrication and Operation of Microfluidic Devices. All microfluidic devices were fabricated by rapid-prototyping soft lithography in PDMS (24). Surfaces of microchannels were made hydrophobic and fluorophilic by silanization (*SI Text*) (25). The chemistrode device was fabricated by inserting connecting Teflon microcapillaries into the 2 arms of a V-shaped channel. Arrays of stimulant plugs were generated by using a microfluidic device according to previously reported procedures (20) or a home-built robotic system (*SI Text*). Gastight syringes (series 1700; Hamilton) with removable 27-gauge needles and 30-gauge Teflon tubing (Weico Wire and Cable) were used to load aqueous solutions and carrier fluid. PHD 2000 infusion syringe pumps (Harvard Apparatus) controlled with LabVIEW (National Instruments) programs were used to drive flows.

Supporting Information. The following procedures are described in *SI Text*: characterization of the temporal and spatial resolution of stimulation and recording by using the chemistrode with fluorescent dyes; analysis of insulin, Ca^{2+}, glucose, and MPTS; and the monitoring of insulin secretion from single mouse islets.

ACKNOWLEDGMENTS. We thank Vytas Bindokas for help with confocal microscopy and Jessica M. Price for contributions in writing and editing this manuscript. This work was supported by National Institutes of Health (NIH) Director's Pioneer Award 1DP1OD003584 and National Science Foundation (NSF) Collaborative Research in Chemistry Grant CHE-0526693 (to R.F.I.), NIH Grants DK48494, DK63493, and DK20595 (to L.H.P.) and the Blum–Kovler Foundation (L.H.P.). R.F.I. is a Cottrell Scholar of Research Corporation and a Camille Dreyfus Teacher–Scholar. A part of this work was performed at the Materials Research Science and Engineering Center microfluidic facility funded by the NSF.

1. Hamill OP, Marty A, Neher E, Sakmann B, Sigworth FJ (1981) Improved patch-clamp techniques for high-resolution current recording from cells and cell-free membrane patches. *Pflugers Arch* 391:85–100.
2. Hubel DH, Wiesel TN (1959) Receptive fields of single neurones in the cats striate cortex. *J Physiol (London)* 148:574–591.
3. Wightman RM (2006) Probing cellular chemistry in biological systems with microelectrodes. *Science* 311:1570–1574.
4. Kennedy RT, Thompson JE, Vickroy TW (2002) In vivo monitoring of amino acids by direct sampling of brain extracellular fluid at ultralow flow rates and capillary electrophoresis. *J Neurosci Methods* 114:39–49.
5. Cellar NA, Burns ST, Meiners JC, Chen H, Kennedy RT (2005) Microfluidic chip for low-flow push–pull perfusion sampling in vivo with on-line analysis of amino acids. *Anal Chem* 77:7067–7073.
6. Stuart JN, Hummon AB, Sweedler JV (2004)The chemistry of thought: Neurotransmitters in the brain. *Anal Chem* 76:120A–128A.
7. El-Ali J, Sorger PK, Jensen KF (2006) Cells on chips. *Nature* 442:403–411.
8. Atencia J, Beebe DJ (2005) Controlled microfluidic interfaces. *Nature* 437:648–655.
9. Sabounchi P, *et al.* (2006) Soft-state biomicrofluidic pulse generator for single cell analysis. *Appl Phys Lett* 88:183901.
10. Anna SL, Bontoux N, Stone HA (2003) Formation of dispersions using ''flow focusing'' in microchannels. *Appl Phys Lett* 82:364–366.
11. Fidalgo LM, Abell C, Huck WTS (2007) Surface-induced droplet fusion in microfluidic devices. *Lab Chip* 7:984–986.
12. Song H, Tice JD, Ismagilov RF (2003) A microfluidic system for controlling reaction networks in time. *Angew Chem Int Ed* 42:768–772.
13. Lorenz RM, Edgar JS, Jeffries GDM, Chiu DT (2006) Microfluidic and optical systems for the on-demand generation and manipulation of single femtoliter-volume aqueous droplets. *Anal Chem* 78:6433–6439.
14. Garstecki P, Fuerstman MJ, Stone HA, Whitesides GM (2006) Formation of droplets and bubbles in a microfluidic T-junction—Scaling and mechanism of break-up. *Lab Chip* 6:437–446.
15. Link DR, *et al.* (2006) Electric control of droplets in microfluidic devices. *Angew Chem Int Ed* 45:2556–2560.
16. Wang M, Roman GT, Schultz K, Jennings C, Kennedy RT (2008) Improved temporal resolution for in vivo microdialysis by using segmented flow. *Anal Chem* 80:5607–5615.
17. Sahoo HR, Kralj JG, Jensen KF (2007) Multistep continuous-flow microchemical synthesis involving multiple reactions and separations. *Angew Chem Int Ed* 46:5704–5708.
18. Song H, Chen DL, Ismagilov RF (2006) Reactions in droplets in microflulidic channels. *Angew Chem Int Ed* 45:7336–7356.
19. Huebner A, *et al.* (2008) Microdroplets: A sea of applications? *Lab Chip* 8:1244–1254.
20. Zheng B, Ismagilov RF (2005) A microfluidic approach for screening submicroliter volumes against multiple reagents by using preformed arrays of nanoliter plugs in a three-phase liquid/liquid/gas flow. *Angew Chem Int Ed* 44:2520–2523.
21. Zheng B, Ismagilov RF (2005) A microfluidic approach for screening submicroliter volumes against multiple reagents by using preformed arrays of nanoliter plugs in a three-phase liquid/liquid/gas flow. *Angew Chem* 117:2576–2579.
22. Adamson DN, Mustafi D, Zhang JXJ, Zheng B, Ismagilov RF (2006) Production of arrays of chemically distinct nanolitre plugs via repeated splitting in microfluidic devices. *Lab Chip* 6:1178–1186.
23. Li L, Boedicker JQ, Ismagilov RF (2007) Using a multijunction microfluidic device to inject substrate into an array of preformed plugs without cross-contamination: Comparing theory and experiments. *Anal Chem* 79:2756–2761.
24. Duffy DC, McDonald JC, Schueller OJA, Whitesides GM (1998) Rapid prototyping of microfluidic systems in poly(dimethylsiloxane). *Anal Chem* 70:4974–4984.
25. Roach LS, Song H, Ismagilov RF (2005) Controlling nonspecific protein adsorption in a plug-based microfluidic system by controlling interfacial chemistry using fluorous-phase surfactants. *Anal Chem* 77:785–796.
26. Tice JD, Song H, Lyon AD, Ismagilov RF (2003) Formation of droplets and mixing in multiphase microfluidics at low values of the Reynolds and the capillary numbers. *Langmuir* 19:9127–9133.
27. Adzima BJ, Velankar SS (2006) Pressure drops for droplet flows in microfluidic channels. *J Micromech Microeng* 16:1504–1510.
28. Bibette J, Calderon FL, Poulin P (1999) Emulsions: Basic principles. *Rep Prog Phys* 62:969–1033.
29. Rekvig L, Frenkel D (2007) Molecular simulations of droplet coalescence in oil/water/surfactant systems. *J Chem Phys* 127.
30. Pawar Y, Stebe KJ (1996) Marangoni effects on drop deformation in an extensional flow: The role of surfactant physical chemistry. 1. Insoluble surfactants. *Phys Fluids* 8:1738–1751.
31. Anderson JR, *et al.* (2000) Fabrication of topologically complex three-dimensional microfluidic systems in PDMS by rapid prototyping. *Anal Chem* 72:3158–3164.
32. Unger MA, Chou HP, Thorsen T, Scherer A, Quake SR (2000) Monolithic microfabricated valves and pumps by multilayer soft lithography. *Science* 288:113–116.
33. Li L, *et al.* (2006) Nanoliter microfluidic hybrid method for simultaneous screening and optimization validated with crystallization of membrane proteins. *Proc Natl Acad Sci USA* 103:19243–19248.
34. Hatakeyama T, Chen DLL, Ismagilov RF (2006) Microgram-scale testing of reaction conditions in solution using nanoliter plugs in microfluidics with detection by MALDI-MS. *J Am Chem Soc* 128:2518–2519.
35. Haustein E, Schwille P (2007) Fluorescence correlation spectroscopy: Novel variations of an established technique. *Annu Rev Biophys Biomolec Struct* 36:151–169.
36. Rocheleau JV, Walker GM, Head WS, McGuinness OP, Piston DW (2004) Microfluidic glucose stimulation reveals limited coordination of intracellular Ca2+ activity oscillations in pancreatic islets. *Proc Natl Acad Sci USA* 101:12899–12903.
37. Ma L, *et al.* (2004) Direct imaging shows that insulin granule exocytosis occurs by complete vesicle fusion. *Proc Natl Acad Sci USA* 101:9266–9271.
38. Dishinger JF, Kennedy RT (2007) Serial immunoassays in parallel on a microfluidic chip for monitoring hormone secretion from living cells. *Anal Chem* 79:947–954.
39. Matsumoto S, Kuroda Y (2002) Perfluorocarbon for organ preservation before transplantation. *Transplantation* 74:1804–1809.
40. Juncker D, Schmid H, Delamarche E (2005) Multipurpose microfluidic probe. *Nat Mater* 4:622–628.
41. Olofsson J, *et al.* (2005) A chemical waveform synthesizer. *Proc Natl Acad Sci USA* 102:8097–8102.
42. Takayama S, *et al.* (2001) Laminar flows—Subcellular positioning of small molecules. *Nature* 411:1016.
43. Chen X, Kis A, Zettl A, Bertozzi CR (2007) A cell nanoinjector based on carbon nanotubes. *Proc Natl Acad Sci USA* 104:8218–8222.
44. Beebe DJ, *et al.* (2000) Functional hydrogel structures for autonomous flow control inside microfluidic channels. *Nature* 404:588–590.
45. Kost J, Langer R (2001) Responsive polymeric delivery systems. *Adv Drug Deliv Rev* 46:125–148.
46. Roeffaers MBJ, *et al.* (2006) Spatially resolved observation of crystal-face-dependent catalysis by single turnover counting. *Nature* 439:572–575.
47. Kastrup CJ, Runyon MK, Shen F, Ismagilov RF (2006) Modular chemical mechanism predicts spatiotemporal dynamics of initiation in the complex network of hemostasis. *Proc Natl Acad Sci USA* 103:15747–15752.
48. Huse M, Lillemeier BF, Kuhns MS, Chen DS, Davis MM (2006) T cells use two directionally distinct pathways for cytokine secretion. *Nat Immunol* 7:247–255.
49. Shea SD, Margoliash D (2003) Basal forebrain cholineraic modulation of auditory activity in the zebra finch song system. *Neuron* 40:1213–1226.
50. Ismagilov RF, Maharbiz MM (2007) Can we build synthetic, multicellular systems by controlling developmental signaling in space and time? *Curr Opin Chem Biol* 11:604–611.